



Parkin overexpression protects from ageing-related loss of muscle mass and strength

Jean-Philippe Leduc-Gaudet^{1,2,3,*} , Olivier Reynaud^{1,2,*}, Sabah N. Hussain³ and Gilles Gousspillou^{1,2,4} 

¹Département des sciences de l'activité physique, Faculté des sciences, Université du Québec à Montréal, Montréal, QC, Canada

²Groupe de recherche en activité physique adaptée, Université du Québec à Montréal, Montréal, QC, Canada

³Department of Critical Care, McGill University Health Centre and Meakins-Christie Laboratories, Department of Medicine, McGill University, Montréal, QC, Canada

⁴Centre de recherche de l'Institut universitaire de gériatrie de Montréal, Montréal, QC, Canada,

Edited by: Michael Hogan & Karyn Hamilton

Key points

- Recent evidence suggests that impaired mitophagy, a process in charge of removing damaged/dysfunctional mitochondria and in part regulated by Parkin, could contribute to the ageing-related loss of muscle mass and function.
- In the present study, we show that Parkin overexpression attenuates ageing-related loss of muscle mass and strength and unexpectedly causes hypertrophy in adult skeletal muscles. We also show that Parkin overexpression leads to increases in mitochondrial content and enzymatic activities. Finally, our results show that Parkin overexpression protects from ageing-related increases in markers of oxidative stress, fibrosis and apoptosis.
- Our findings place Parkin as a potential therapeutic target to attenuate sarcopenia and improve skeletal muscle health and performance.

Abstract The ageing-related loss of muscle mass and strength, a process called sarcopenia, is one of the most deleterious hallmarks of ageing. Solid experimental evidence indicates that mitochondrial dysfunctions accumulate with ageing and are critical in the sarcopenic process. Recent findings suggest that mitophagy, the process in charge of the removal of damaged/dysfunctional mitochondria, is altered in aged muscle. Impaired mitophagy represents an attractive mechanism that could contribute to the accumulation of mitochondrial dysfunctions and sarcopenia. To test this hypothesis, we investigated the impact of Parkin overexpression in skeletal muscles of young and old mice. Parkin was overexpressed for 4 months in muscles of young (3 months) and late middle-aged (18 months) mice using i.m. injections of adeno-associated viruses. We show that Parkin overexpression increased muscle mass, fibre size and mitochondrial

Jean-Philippe Leduc-Gaudet obtained a BSc in Kinesiology and completed a MSc in Exercise Physiology at UQAM (Montréal, Canada). During his MSc, his research focused on the impact of nutrition on mitochondrial energetics in skeletal muscle. He is currently a PhD candidate under the supervision of Dr Gilles Gousspillou and Dr Sabah Hussain at the Meakins-Christie Laboratories affiliated to McGill University (Montréal, Canada). His research now focuses on the investigation of the role played by mitochondrial quality control in muscle health, ageing and diseases. **Olivier Reynaud** obtained a BSc in Molecular Biology and completed a MSc in Exercise Physiology at UQAM under the supervision of Dr Gilles Gousspillou. His research interests are in the field of molecular biology, with a particular focus on skeletal muscle physiology and mitochondrial biology in ageing and disease. He now works as a research assistant in Dr Gilles Gousspillou's laboratory.



*These authors contributed equally to this work.

enzyme activities in both young and old muscles. In old mice, Parkin overexpression increased muscle strength, primordial germ cell-1 α content and mitochondrial density. Parkin overexpression also attenuated the ageing-related increase in 4-hydroxynonenal content (a marker of oxidative stress) and type I collagen content (a marker of fibrosis), as well as the number of terminal deoxynucleotidyl transferase dUTP nick-end labelling-positive myonuclei (a marker of apoptosis). Overall, our results indicate that Parkin overexpression attenuates sarcopenia and unexpectedly causes hypertrophy in adult muscles. They also show that Parkin overexpression leads to increases in mitochondrial content and enzymatic activities. Finally, our results show that Parkin overexpression protects against oxidative stress, fibrosis and apoptosis. These findings highlight that Parkin may be an attractive therapeutic target with respect to attenuating sarcopenia and improving skeletal muscle health and performance.

(Received 14 September 2018; accepted after revision 21 December 2018; first published online 7 January 2019)

Corresponding author G. Gousspillou, Département des sciences de l'activité physique, Faculté des sciences, Université du Québec à Montréal (UQAM), Pavillon des sciences biologiques (SB), Local: SB-4640, 141, Avenue du Président Kennedy, Montréal, Québec, H2X 1Y4, Canada. Email: gousspillou.gilles@uqam.ca

Introduction

One of the most deleterious hallmarks of ageing is the progressive decline of muscle mass and function, a process called sarcopenia. Sarcopenia can have dramatic consequences for afflicted individuals because it progressively leads to mobility impairment, falls and physical frailty (Janssen *et al.* 2002; Deschenes, 2004; Janssen *et al.* 2004a; Kim & Choi, 2013). In addition, sarcopenia represents a major burden for various societies. It is estimated that the prevalence of sarcopenia increases from 14% in 65–70-year-olds to over 50% in those above 80 years old (Santilli *et al.* 2014). The number of people around the world aged over 60 years was estimated at 600 million in the year 2000 and is expected to rise to 1.2 billion by 2025 and to 2 billion by 2050. Even with a very conservative estimate of prevalence, sarcopenia currently affects over 50 million people worldwide and will affect over 200 million in the next 30 years (Santilli *et al.* 2014). Furthermore, the direct healthcare costs attributable to sarcopenia and its sequela are considerable, estimated at 18.5 billion dollars for 2000 alone in the USA (Janssen *et al.* 2004b). Developing effective therapeutic interventions to counteract sarcopenia is therefore one of the major challenges facing health research.

There is strong evidence that accumulation of dysfunctional mitochondria plays an important role in the skeletal muscle ageing process. Notably, aged skeletal muscles display impaired mitochondrial energetics (Trounce *et al.* 1989; Short *et al.* 2005; Gousspillou *et al.* 2010; Lanza *et al.* 2012; Gousspillou *et al.* 2014a) and increased mitochondrial-mediated apoptosis (Selman *et al.* 2003; Dirks & Leeuwenburgh, 2004; Leeuwenburgh *et al.* 2005; Chabi *et al.* 2008; Marzetti *et al.* 2008; Picard *et al.* 2010; Picard *et al.* 2011; Gousspillou *et al.* 2014b). Furthermore, overexpression of a mitochondrial-targeted catalase (antioxidant enzyme) has been shown to attenuate

the effect of ageing on skeletal muscle, thereby supporting a causal role for mitochondrial dysfunction in the sarcopenic process (Umanskaya *et al.* 2014). In addition, the two most efficient non-pharmacological strategies to attenuate the effects of ageing on skeletal muscle, calorie-restriction (Mayhew *et al.* 1998; Baker *et al.* 2006; Hepple *et al.* 2006) and endurance training (Coggan *et al.* 1992; Song *et al.* 2006), are known to improve mitochondrial function (Gousspillou & Hepple, 2013).

Although the mechanisms underlying this ageing-related accumulation of dysfunctional mitochondria are not yet fully understood, recent evidence indicates that reduced mitophagy may play a causal role (O'Leary *et al.* 2013; Gousspillou *et al.* 2014b). Mitophagy is the selective removal of dysfunctional mitochondria by autophagosomes. This process is regulated to a large extent by the Parkin–Pink1 pathway, which plays an important role in maintaining mitochondrial quality in skeletal muscles by selectively removing dysfunctional and depolarized mitochondria (Narendra *et al.* 2008). In the context of muscle ageing, it has been reported that the ratio of Parkin to VDAC (voltage-dependent anion channel; a protein recruiting Parkin to dysfunctional mitochondria for the initiation of mitophagy) (Sun *et al.* 2012) is significantly reduced in atrophied muscle of old men (Gousspillou *et al.* 2014b). In addition, it has been reported that autophagy-related genes, such as BNIP3, BECLIN-1, ATG7 and PARK2 (the gene coding for Parkin), are downregulated in inactive older women (Drummond *et al.* 2014). Interestingly, skeletal muscles from adult Parkin knockout mice display some ageing-like features, including contractile dysfunction, impaired mitochondrial energetics and a sensitization of the apoptosis-regulating mitochondrial permeability transition pore (Gousspillou *et al.* 2018). In line with these findings, it was shown that inhibition of mitophagy by selectively deleting autophagy-related genes

causes mitochondrial dysfunction and muscle atrophy (Masiero *et al.* 2009; Carnio *et al.* 2014). By contrast, Parkin overexpression in *Drosophila* skeletal muscle was shown to increase mitochondrial content and attenuate the accumulation of protein aggregates, a marker of cellular ageing (Rana *et al.* 2013). Altered mitophagy with ageing therefore represents a potential mechanism that could lead to an accumulation of mitochondrial dysfunctions and, in turn, to sarcopenia.

To test the hypothesis, we overexpressed Parkin, a key regulator of mitophagy, for 4 months in skeletal muscles of young and late middle-aged mice using *i.m.* injections of adeno-associated viruses (AAV). We found that Parkin overexpression in adult skeletal muscle results in muscle hypertrophy and an increase in mitochondrial enzyme activities. We also showed that overexpression of Parkin in aged mice increases muscle mass, muscle strength, mitochondrial content and enzymatic activity, at the same time as lowering markers of oxidative stress, fibrosis and apoptosis. Taken altogether, these results indicate that Parkin is a potential therapeutic target to attenuate sarcopenia and improve skeletal muscle health and performance.

Methods

Ethical approval

The present study was carried out in strict accordance with standards established by the Canadian Council of Animal Care and the guidelines and policies of UQAM. All procedures were approved by the animal ethics committees of UQAM (#CIPA883). Experimental protocols were designed to minimize suffering and the number of animals used in the study. The authors declare that their work complies with the ethical principles under which *The Journal of Physiology* operates (Grundy, 2015).

Animal procedures and AAV injection

Experiments were conducted on 3-month-old (purchased from Jackson Laboratories, Bar Harbor, ME, USA) and 18-month-old (obtained through the Quebec Research Network on Aging, Montreal, QC, Canada) male C57BL/6J mice. Three to four mice were housed per cage under a 12:12 h light/dark photocycle at $24 \pm 1^\circ\text{C}$ and 50–60% relative humidity with access to standard chow diet and water available *ad libitum*. All AAV used in the present study were purchased from Vector Labs (Burlingame, CA, USA) and were of Serotype 1, which is a serotype with a proven tropism for skeletal muscle cells. After a 3-day acclimatization period, an AAV containing a muscle specific promoter (muscle creatine kinase), a sequence coding for the reporter protein green fluorescent

protein (GFP) and a sequence coding for Parkin (details on the AAV construction are available in Fig. 1A) were injected *i.m.* ($25 \mu\text{L}$ per site; 2.5×10^{11} gc) into the right tibialis anterior (TA) and gastrocnemius (GAS) muscles. In this construction, the sequences coding for Parkin and GFP were separated by a sequence coding for the auto-cleavable 2A peptide, allowing the separation of Parkin and GFP once translated. A control AAV containing only the GFP sequence under the control of the MCK promoter was injected into the contralateral leg. Injections were carried out under general anaesthesia using 2% isoflurane. Because the AAVS1 recombination site in wild-type AAV was deleted in these recombinant AAVs, both GFP and Parkin expression comprised episomal expression without integration into the host DNA. Two AAV injections, separated by 2 months, were therefore performed to ensure that Parkin expression remained elevated throughout the duration of the study. The first sets of *i.m.* injection were performed at 3 and 18 months, with the second set at 5 and 20 months. After 4 months of Parkin and/or GFP overexpression, mice either underwent a protocol to assess muscle contractile function or were anaesthetized with isoflurane and subsequently killed by cervical dislocation. For mice killed by cervical dislocation, the TA and GAS from both legs were removed. The TA and GAS were cut in half; one-half was mounted for histology as described in (Gouspillou *et al.* 2014c; Leduc-Gaudet *et al.* 2015). Small strips from the white GAS were prepared for analyses by transmission electron microscopy (TEM). The rest of the TA and GAS were frozen in liquid nitrogen and stored -80°C until use for western blot and quantitative PCR experiments.

In situ assessment of muscle contractile function

Mice were anaesthetized with an *i.p.* injection of a ketamine-xylazine cocktail (ketamine: 130 mg kg^{-1} ; xylazine: 20 mg kg^{-1}). Anaesthesia was maintained with supplemental doses of 0.05 mL as needed. The surgical procedure and *in situ* contractile stimulation protocol were performed as described previously, with minor modifications (Mofarrahi *et al.* 2015). The distal tendon of the left and right TA muscle was isolated and attached in turn with surgical 4.0 silk to the lever arm of a 305C-LR servomotor (Aurora Scientific Instruments, Aurora, ON, Canada). The Dynamic Muscle Control and Analysis Software Suite (Aurora Scientific Instruments) was used for collection and data analysis. The partially exposed muscle surface of the TA was kept moist for the contractile stimulation protocol and was directly stimulated with an electrode placed on the belly of the muscle. *In situ* measurement of the TA with direct stimulation was chosen over sciatic nerve stimulation, thereby removing potential negative effects such as a central contribution and, because

blood delivery is intact, eliminating potential problems of isolated muscles (Allen *et al.* 2008). Optimal muscle length and voltage was progressively adjusted to produce maximal tension. The pulse duration was set to 0.2 ms for all tetanic contractions. Force–frequency relationships curves were determined at muscle optimal length at 10, 30, 50, 70, 100, 120 and 150 Hz, with 1 min intervals between stimulations to avoid fatigue.

Skeletal muscle sample sectioning for histology

Cross-sections (thickness 10 μm) were cut in a cryostat at -18°C and mounted on lysine coated slides (Superfrost; Thermo Fisher, Waltham, MA, USA) to determine AAV transduction efficiency, muscle fibre size, succinate dehydrogenase (SDH) and cytochrome *c* oxidase (COX) activities, the proportion of terminal deoxynucleotidyl transferase dUTP nick-end labelling (TUNEL) positive myonuclei, as well as the content of primordial germ cell (PGC)-1 α , type I collagen and 4-hydroxynonenal (HNE) using immunohistological procedures described previously (Gospillou *et al.* 2014c; Leduc-Gaudet *et al.* 2015). These sections were also used to assess transduction efficiency of AAVs.

Assessment of AAV transduction efficiency

Because both AAVs used in the present study contained a sequence coding for GFP, transduction efficiency was assessed by simply examining the proportion of GFP positive fibres on muscle cross-sections. Accordingly, slides were removed from our -80°C freezer and directly cover slipped using ProlongDiamond (Thermo Fisher) as mounting medium. Slides were then immediately imaged with an Axio 2 imager microscope (Carl Zeiss, Oberkochen, Germany) using a GFP fluorescence filter. A control slide obtained from a TA of a 3-month-old control (i.e. no AAV injection) mouse was used to confirm that all image acquisition parameters were not yielding the detection of autofluorescence. Once all of the acquisition parameters were set, with no detectable signal on the control slide, all slides were imaged using the exact same settings.

In situ determination of fibre size

Muscle cross-sections were immunolabelled for laminin. Briefly, muscle cross-sections were first allowed to reach

Table 1. Number of fibres analysed to quantify the impact of ageing and Parkin overexpression on muscle fibre size

	TA	GAS
7mo-AAV-GFP	504 \pm 135	298 \pm 26
7mo-AAV-Parkin	452 \pm 88	296 \pm 33
22mo-AAV-GFP	658 \pm 157	303 \pm 6
22mo-AAV-Parkin	614 \pm 266	289 \pm 29

Data are presented as the mean \pm SD.

room temperature and rehydrated with PBS (pH 7.2) and then blocked with goat serum (10% in PBS). Sections were then incubated with primary rabbit immunoglobulin (Ig)G polyclonal anti-laminin antibody (L9393; Sigma, St Louis, MO, USA; dilution 1:750) for 1 h at room temperature. Sections were washed three times in PBS before being incubated for 1 h at room temperature with an Alexa Fluor 594 goat anti-rabbit IgG antibody (A-11037; Invitrogen, Carlsbad, CA, USA; dilution 1:100). Sections were then washed three times in PBS and slides were cover slipped using Prolong Gold (P36930; Invitrogen) as mounting medium. Slides were imaged with a fluorescence microscope (Zeiss Axio Imager 2). The average number of fibres analysed is presented in Table 1.

In situ determination of PGC-1 α , type I collagen and 4-HNE content

For each sample, muscle cross-sections were immunolabelled to assess PGC-1 α , type I collagen and 4-HNE content *in situ*. Sections were first allowed to reach room temperature and were fixed in acetone at 4°C for 15 min (Gospillou *et al.* 2014c), a step causing the loss of GFP fluorescence. Samples were then washed for 5 min in PBS (pH 7.4) at 4°C before being incubated for 15 min in a permeabilization solution (0.1% Triton X-100 in PBS) at 4°C (Gospillou *et al.* 2014c). Slides were then washed three times in PBS before being incubated at 4°C in a blocking solution (10% goat serum in PBS) for 30 min at room temperature (Gospillou *et al.* 2014c). Slides were then incubated for 60 min at room temperature with a rabbit IgG polyclonal anti-PGC-1 α antibody (Ab3242; Abcam, Cambridge, MA, USA; dilution 1:50), a rabbit polyclonal antibody anti-type I collagen (Ab34710; Abcam; dilution 1:50) or a mouse monoclonal anti-4HNE antibody (#HNE 13-M; Alpha Diagnostic International, San Antonio, TX,

is shown to decline with ageing and injection of AAV-Parkin results in successful Parkin overexpression. *F*, fold change in Parkin expression in young and old GAS induced by AAV-Parkin injection. The graph shows successful Parkin overexpression. *G*, western blot detection and quantification of the ubiquitin content in the TA of old mice injected with either AAV-Parkin or AAV-GFP. Parkin overexpression is shown to result in a significant increase in protein ubiquitination. *Statistically significant. [Colour figure can be viewed at wileyonlinelibrary.com]

USA; dilution 1 :100) (Gouspillou *et al.* 2014c). For PGC-1 α immunolabelling, sections were also incubated with a mouse IgG monoclonal anti-dystrophin antibody (D8168; Sigma; dilution 1:100). Slides were then washed three times in PBS at 4°C before being incubated for 60 min at room temperature with an Alexa Fluor 488 IgG goat anti-mouse antibody (A-11001; Invitrogen; dilution 1:500), an Alexa Fluor 594 goat anti-mouse IgG, (A-21235; Invitrogen; dilution 1:100) and/or an Alexa Fluor 594 goat anti-rabbit IgG antibody (A-11037; Invitrogen; dilution 1:100) (Gouspillou *et al.* 2014c). Slides were then washed three times in PBS. For PGC-1 α immunolabelling, sections were then incubated for 10 min in a PBS solution containing 4',6-diamidino-2-phenylindole (DAPI) (D1306; Invitrogen; [300 nm]) at 4 °C and subsequently washed three times in PBS. Sections were finally cover slipped using Prolong Gold (P36930; Invitrogen) as mounting medium (Gouspillou *et al.* 2014c). Images of cross-sections were then taken with a fluorescence microscope (Zeiss Axio Imager 2) and analysed using ImageJ (NIH, Bethesda, MD, USA).

In situ determination of SDH and COX activities

Muscle cross-sections were stained for SDH (complex II of the respiratory chain) and COX (complex IV of the respiratory chain) activity as described previously (Gouspillou *et al.* 2014c; Leduc-Gaudet *et al.* 2015; St-Jean-Pelletier *et al.* 2017). Briefly, sections were first allowed to reach room temperature and were rehydrated with PBS (pH 7.2). Sections were then incubated in a solution containing nitroblue tetrazolium (1.5 mM; 11585029001; Sigma), sodium succinate (130 mM; S2378; Sigma), phenazine methosulphate (0.2 mM; P9625; Sigma) and sodium azide (0.1 mM) for SDH activity or in a solution containing cytochrome *c* (100 μ M; C7752; Sigma) and 3,3'-diaminobenzidine tetrahydrochloride (4 mM; D5637; Sigma) for 20 min at 37°C. Cross-sections were then washed three times in PBS and cover-slipped using an aqueous mounting medium (VectaMount AQ Medium, H-5501; Vector Labs). All samples were processed at the same time and using the same incubation solution, ensuring that all samples underwent the exact same conditions.

Detection of apoptosis by TUNEL

The presence of 180–200 bp DNA fragments, obtained during genome fragmentation by endonucleases (Kyrylkova *et al.* 2012), is a robust marker of cellular apoptosis. TUNEL is a detection method used to locate these DNA fragments generated during apoptosis. In the present study, apoptotic myonuclei were detected using a commercial TUNEL kit (catalogue number

11684795910; Roche, Basel, Switzerland) in accordance with the manufacturer's instructions. Sections were also incubated for 1 h at room temperature with a mouse IgG monoclonal anti-dystrophin antibody (D8168; Sigma; dilution 1:100), followed by a 1 h incubation at room temperature with an Alexa Fluor 647 goat anti-mouse IgG antibody (A-21235; Invitrogen; dilution 1:100). Sections were finally incubated for 10 min in a PBS solution containing DAPI (D1306; Invitrogen; [300 nm]) at 4 °C, washed three times in PBS and cover slipped using Prolong Gold (P36930; Invitrogen) as mounting medium. Images were acquired using a fluorescence microscope (Zeiss Axio Imager 2) and analysed using ImageJ (NIH).

Immunoblotting

Approximately 20 mg of each TA was homogenized in 10 volumes of an extraction buffer composed of 50 mM Tris base, 150 mM NaCl, 1% Triton X-100, 0.5% sodium deoxycolate, 0.1% SDS and 10 μ L mL⁻¹ of a protease inhibitor cocktail (P8340; Sigma). The homogenate was centrifuged at 15,000 g for 15 min at 4°C. Protein content in the supernatant was determined using the Bradford method with BSA as standard.

Aliquots of supernatant were mixed with Laemmli buffer and subsequently boiled at 95°C for 5 min. Equal amounts (20 μ g) of proteins were loaded onto 8–12% gels, electrophoresed by SDS-PAGE and transferred to polyvinylidene fluoride membranes (Trans-blot Turbo Midi-size LF PVDF Membrane; Bio-Rad, Hercules, CA, USA). Membranes were incubated for 1 h at room temperature in a blocking buffer composed of Tris-buffered saline containing 5% non-fat dried milk and 0.1% Tween 20 (TBS-T) and probed either overnight at 4 °C or for 1 h at room temperature with the primary antibodies: mouse monoclonal antiPRK8 (Parkin; sc32282; Santa Cruz Biotechnology, Santa Cruz, CA, USA), mouse monoclonal anti-S6 ribosomal protein (54D2; #2317; Cell Signaling Technology, Beverly, MA, USA; dilution 1:500), rabbit polyclonal anti-phospho-S6 ribosomal protein (Ser240/244) (#2215; Cell Signaling; dilution 1:500), mouse monoclonal anti-4-HNE (MAB3249; Bio-Techne, Minneapolis, MN, USA; dilution 1:500) and a mouse monoclonal anti-ubiquitin (Ub P4D1; sc-8017; Santa Cruz Biotechnology) diluted in blocking buffer. Membranes were washed (6 \times 5 min) in TBS-T and subsequently incubated with appropriated HRP-conjugated secondary antibodies (Ab6721; Abcam; dilution 1:5000; and Ab6728, Abcam; dilution 1:5000) diluted in blocking buffer for 1 h at room temperature. Protein signals were detected using enhanced chemiluminescence substrate (24080; Thermo Fisher), imaged with the ChemiDoc Touch Imaging System (Bio-Rad).

TEM

The assessment of mitochondrial density and area was performed using TEM as described previously (Picard *et al.* 2013a; Picard *et al.* 2013b). Small stripes prepared from white GAS were incubated in 2% glutaraldehyde buffer solution in 0.1 M cacodylate (pH 7.4) and subsequently post-fixed in 1% osmium tetroxide in 0.1 M cacodylate buffer, dehydrated in increasing concentrations of ethanol and propylene oxide, and embedded in epon. Sections (thickness 1 μm) were stained with toluidine blue to confirm the orientation of the muscle tissue prior the ultrathin sectioning. Ultrathin sections were cut in longitudinal or transverse orientation using an Ultracut S ultramicrotome (Leica Microsystems, Wetzlar, Germany) and mounted on nickel carbon-formvar coated grids. Uranyl acetate and lead citrate stained sections were imaged using a Philips CM100 electron microscope (FEI, Hillsboro, OR, USA). Digital micrographs were captured using an XR80 CCD digital camera (Advanced Microscopy Techniques, Woburn, MA, USA) at 7900 \times magnification. Individual intermyofibrillar mitochondria from four old GFP expressing and four old Parkin overexpressing white GAS were manually traced in longitudinal orientations using ImageJ (NIH) to quantify the average area of individual mitochondria (in μm^2) and mitochondrial density (i.e. the percentage of the cytoplasmic surface occupied by mitochondria).

Quantitative real-time PCR

Total RNA was extracted from frozen GAS muscles using a PureLinkTM RNA Mini Kit (Invitrogen Canada, Burlington, ON, Canada). Total RNA (2 μg) was reverse transcribed using a Superscript II[®] Reverse Transcriptase Kit and random primers (Invitrogen Canada). Reactions were performed at 42°C for 50 min and at 90°C for 5 min. Real-time PCR detection of mRNA expression was performed using a Prism[®] 7000 Sequence Detection System (Applied Biosystems, Foster City, CA, USA). Real-time PCR experiments were performed in triplicate. Relative mRNA quantifications of the Park2 gene were determined using the threshold cycle ($\Delta\Delta\text{CT}$) method using the housekeeping gene cyclophilin. The primer sequences for Park2 and cyclophilin mRNA amplification were: mouse Park2: 5'-TCTTCCAGTGTAACCACCGTC-3' and 5'-GGCAGGGAGTAGCCAAGTT-3'; mouse cyclophilin: 5'-GCGTCTCCTTCGAGCTGTTT-3' and 5'-CTGGCACATGAATCCTGGAAC-3'.

Statistical analysis

The effects of ageing on parameters of interest were assessed by comparing 7mo-AAV-GFP and 22mo-AAV-GFP using bilateral unpaired *t* tests, with the

exception of the impact of ageing on fibre size distribution, which was tested using two-way ANOVA. When data for all four groups (i.e. 7mo-AAV-GFP, 7mo-AAV-Parkin, 22mo-AAV-GFP and 22mo-AAV-Parkin) were available, the effects of Parkin overexpression on parameters of interest were assessed using two-way repeated measures ANOVA. Differences between 7mo-AAV-GFP and 7mo-Saline were tested using bilateral unpaired *t* tests. When data were available for only one group of age (i.e. either 7mo-AAV-GFP + 7mo-Parkin or 22mo-AAV-GFP + 22mo-AAV-Parkin), comparisons involving one variable were performed using bilateral paired *t* tests. When data were available for only one group of age but multiple comparisons were performed (e.g. force–frequency relationship) differences were tested using two-way repeated measures ANOVA (to assess the impact of Parkin overexpression). For all ANOVA and *t* tests, $P < 0.5$ was considered statistically significant. Correction for multiple comparisons following two-way ANOVA and two-way repeated measures ANOVA were performed using the two-stage step-up method of Benjamini, Krieger and Yekutieli (Benjamini *et al.* 2006; $q < 0.1$ was considered statistically significant). All statistical analyses were performed using Prism, version 7 (GraphPad Software Inc., San Diego, CA, USA).

Results

Successful overexpression of Parkin using i.m. AAV injections

Parkin overexpression in the TA and GAS was achieved via i.m. injections of AAVs expressing mouse PARK2 and GFP under the control of a muscle specific promoter (muscle creatine kinase) (Fig. 1A and B). Control AAVs expressing GFP were injected into the muscles of the contralateral leg (Fig. 1B). Our experimental design provides an important advantage in that each animal is its own control. This is particularly relevant to the issue of muscle ageing because ageing-related changes in nutritional intake, hormonal status, physical activity and systemic inflammation can all influence sarcopenia (Tieland *et al.* 2018). In young adult mice, Parkin overexpression was initiated at 3 months of age (after the developmental phase) to avoid any potential impact of its overexpression on muscle development. In the old group, Parkin overexpression was initiated at 18 months of age because muscle atrophy is not yet detectable at that time point (Hwee *et al.* 2014). Animals were studied after 4 months of Parkin and/or GFP overexpression (at the ages of 7 or 22 months, respectively) (Fig. 1C). As shown in Fig. 1D, AAV transduction efficiency was almost 100% (all fibres were GFP-positive) for all samples examined. Injection of AAV-Parkin significantly increased muscle Parkin mRNA expression and protein content in both young and old mice

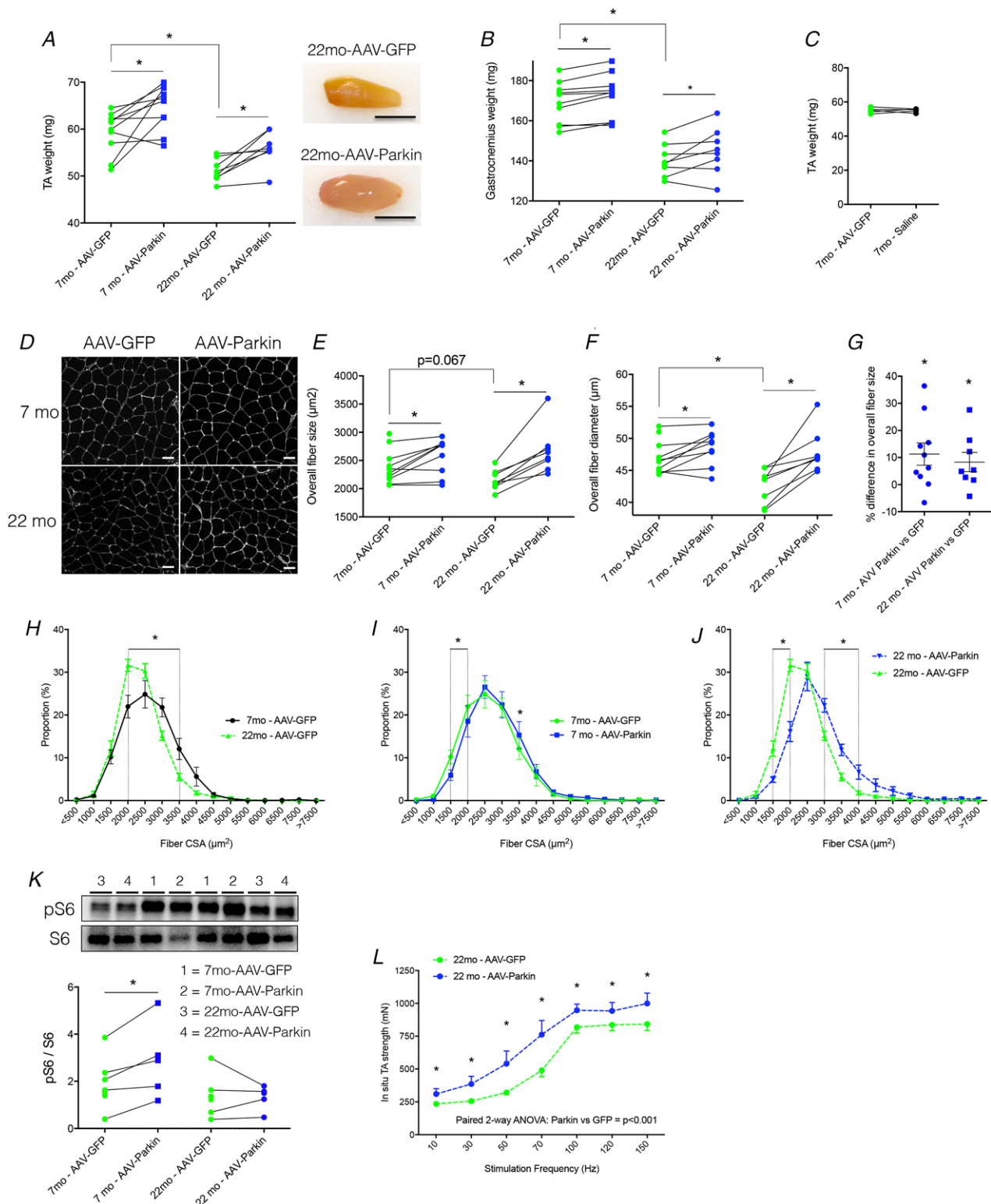


Figure 2. AAV-mediated overexpression of Parkin increases muscle weight and fibre size in young mice and attenuates sarcopenia

A and *B*, quantification of the impact of ageing and Parkin overexpression on TA (*A*) and GAS (*B*) weights. Ageing is shown to be associated with significant muscle atrophy (7mo-AAV-GFP ($n = 10$) vs. 22mo-AAV-GFP). Parkin overexpression results in higher muscle mass in both young and old muscles vs. their GFP expressing counterparts. Also shown in (*A*) are representative images demonstrating that old muscles injected with AAV-Parkin are bigger than muscles injected with AAV-GFP (scale bars = 5 mm). *C*, quantification of the effect of GFP expression on the

(Fig. 1E and F). Importantly, we observed that endogenous Parkin protein content was significantly lower in old as compared to young TA, indicating that muscle Parkin content declines with ageing (Fig. 1E). In line with the ubiquitin E3 ligase activity of Parkin, immunoblotting for ubiquitin protein conjugates confirmed that Parkin overexpression significantly increases overall muscle protein ubiquitination (Fig. 1G).

Parkin overexpression triggers hypertrophy in young mice and attenuates ageing-related loss of muscle mass and strength

To test the hypothesis that Parkin overexpression in old muscle will attenuate sarcopenia, we measured the impact of ageing in the absence and presence of Parkin overexpression on muscle mass and fibre size. In the absence of Parkin overexpression, muscles of old mice demonstrated clear signs of fibre atrophy, including decreased muscle mass and fibre size, compared to muscles of young mice (Fig. 2A–H). Parkin overexpression in both young and old mice resulted in significant increases in muscle weight (Fig. 2A and B) and fibre size (Fig. 2D–J). We should emphasize that prolonged overexpression of GFP (4 months) had no effect on muscle weight (Fig. 2C). To assess whether the increase in muscle weight and fibre size in response to Parkin overexpression is mediated by an increase in the activity of the Akt-mTORC1 pathways, we quantified the extent of S6 protein phosphorylation as an index of mTORC1 activation. Figure 2K shows that Parkin overexpression was associated with significant increases in S6 protein phosphorylation in young but not old skeletal muscles.

To define whether the greater muscle fibre size and muscle mass seen in Parkin overexpressing muscle was translating into functional gain, we next assessed *in situ* TA strength in old mice. Accordingly, a new batch of

old mice was used. Importantly, this second batch of animals allowed us to replicate our original findings on the impact of Parkin overexpression on the TA weight (data not shown). Overexpression of Parkin was associated with a significant increase in force generation at any given stimulation frequency compared to GFP overexpression (Fig. 2L).

Parkin overexpression increases mitochondrial enzyme activity and mitochondrial content

Because Parkin is well known for its role in mitochondrial quality control processes, we investigated whether the positive impact of Parkin overexpression on muscle mass and function was associated with changes in mitochondrial enzymatic activities and mitochondrial content. Parkin overexpression significantly increased the activities of SDH and COX (complexes II and IV of the electron transfer system) (Fig. 3A–D). Measurement of muscle mitochondrial density with TEM confirmed that Parkin overexpression in old muscles significantly increased mitochondrial density by 72% compared to GFP overexpression (Fig. 3E and F). Interestingly, this increase in mitochondrial density was associated with a significant decrease in the average area of individual mitochondria (Fig. 3G). To determine whether the changes in mitochondrial enzyme functions and mitochondrial density elicited by Parkin overexpression were the result of increased mitochondrial biogenesis, we quantified PGC-1 α expression using immunostaining of muscle cross-sections (Fig. 3H). We found that normal ageing is associated with a trend for a decrease in PGC-1 α expression, which is a finding consistent with previous studies (Baker *et al.* 2006; Chabi *et al.* 2008; Joseph *et al.* 2012). Parkin overexpression elicited a significant increase in PGC-1 α expression in old but not young skeletal muscles (Fig. 3H and I).

weight of the TA in young mice. The graph shows that GFP expression did not alter TA weight. D, representative laminin immunolabelling performed on muscle cross-sections of young and old GAS muscles expressing either GFP or Parkin. E and F, quantification of the impact of ageing and Parkin overexpression on average gastrocnemius fibre size (E) and minimal Feret diameter (F). The graphs show that ageing is associated with myofibre atrophy, whereas Parkin overexpression results in a higher fibre size in both young ($n = 10$ AAV-GFP; $n = 9$ AAV-Parkin) and old ($n = 8$) mice (scale bar = 50 μ m). G, quantification of the impact of Parkin on TA fibre size in young and old mice. Parkin overexpressing TA also demonstrated larger fibres vs. their GFP expressing counterparts. H, quantification of the effect of ageing on GAS fibre size distribution between young ($n = 9$) and old ($n = 8$) mice. The graph shows a distributional shift to the left in aged muscles, a clear sign of atrophy. I, quantification of the effect of Parkin overexpression on GAS fibre size distribution in young ($n = 9$) mice. The graph shows a distributional shift to the right in Parkin overexpressing muscle, indicating hypertrophy. J, quantification of the effect of Parkin overexpression on GAS fibre size distribution in old ($n = 8$) mice. The graph shows a distributional shift to the right in old Parkin overexpressing muscle, clearly showing that old Parkin overexpressing muscles have larger fibres vs. their GFP expressing counterparts. K, western blot detection and quantification of pS6 and S6 content in the TA of young and old GFP expressing or Parkin overexpressing muscles. Also shown in (K) is a quantification of the pS6 to S6 ratio, a marker of the Akt-mTOR pathway activity. The graph shows that Parkin overexpression increased the pS6 to S6 ratio only in young muscles. L, quantification of the strength/stimulation frequency relationship in old AAV-GFP ($n = 5$) and AAV-GFP-Parkin ($n = 5$) injected muscles showing that Parkin expression increased muscle strength for all of the stimulation frequencies we tested. *Statistically significant. [Colour figure can be viewed at wileyonlinelibrary.com]

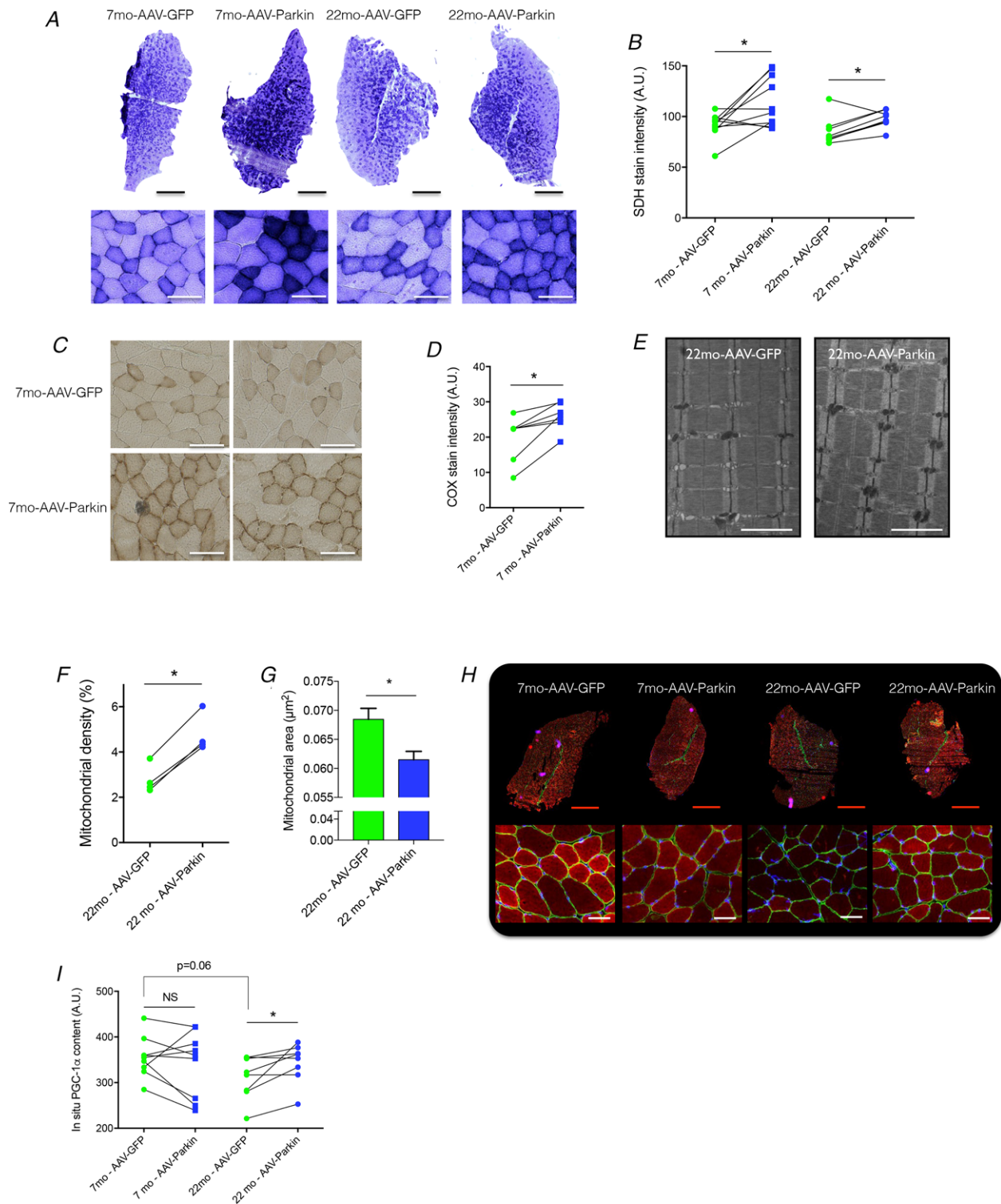


Figure 3. Parkin overexpression increases mitochondrial enzyme activity and mitochondrial content
 A and B, representative SDH stains (A) performed on muscle cross-sections of young and old muscles expressing either GFP or Parkin. Whole cross-sections stained for SDH are shown in the first row of images, whereas representative images obtained at a higher magnification are shown in the second row (black scale bars = 1000 μm ; white scale bars = 100 μm). B, corresponding quantification of SDH stain intensity, which is proportional to SDH activity. The quantification reveals that Parkin overexpression increases SDH activity in both young ($n = 10$) and old ($n = 8$) muscles. C and D, representative COX stains (C) performed on muscle cross-sections of young muscles expressing either GFP or Parkin and corresponding quantification (D) of COX stain intensity, which is proportional

to COX activity (scale bar = 100 μm). The quantification reveals that Parkin overexpression increased COX activity in young muscles ($n = 7$ per group). *E–G*, representative TEM images (*E*) of old GFP expressing and Parkin overexpressing muscles (scale bar = 2 μm). From such TEM images, the mitochondrial volume density (*F*) and the average size of individual mitochondria (*G*) were quantified. *F* and *G*, Parkin overexpression in old muscles increased mitochondrial density (*F*) ($n = 4$ per group) at the same time as decreasing the size of individual mitochondria (*G*) (22mo-AAV-GFP: $n = 586$ mitochondria; 22mo-AAV-Parkin: $n = 666$ mitochondria; unpaired bilateral *t* test). *H* and *I*, representative *in situ* immunolabelling of PGC-1 α (red), dystrophin (green) and nuclei (blue) (*H*) performed in young ($n = 9$) and old ($n = 8$) muscles expressing GFP or overexpressing Parkin. Whole cross-sections are shown in the first row of images, whereas representative images obtained at a higher magnification are shown in the second row (red scale bars = 1000 μm ; white scale bars = 50 μm). *I*, corresponding quantification of PGC-1 α immunolabelling intensity showing a trend for decreased PGC-1 α content with ageing and increased PGC-1 α content induced by Parkin overexpression in old mice. *Statistically significant. NS, not significant. [Colour figure can be viewed at wileyonlinelibrary.com]

Parkin overexpression attenuates ageing-related oxidative stress

Oxidative stress has been consistently detected in aged skeletal muscle and is considered to contribute to ageing-related decreases in muscle mass and function (Yan & Sohal, 1998; Capel *et al.* 2005; Yarian *et al.* 2005; Chabi *et al.* 2008; Sohal & Orr, 2012; Sinha-Hikim *et al.* 2013; Umanskaya *et al.* 2014). To assess whether

Parkin overexpression may affect the development of oxidative stress in old muscles, we assessed muscle content of 4-HNE (i.e. a marker of lipid peroxidation) using immunostaining and immunoblotting. Figure 4 shows that normal ageing is associated with a significant increase in muscle 4-HNE content. Parkin overexpression elicited a significant decrease in 4-HNE content in old but not young skeletal muscles (Fig. 4). These results indicate that

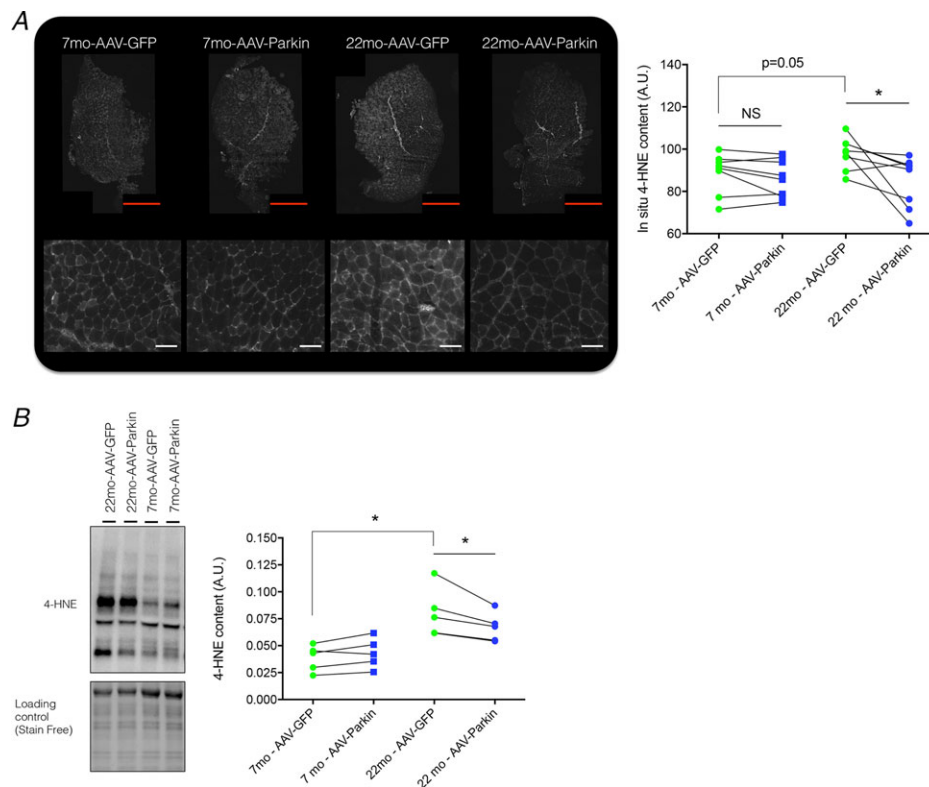


Figure 4. Parkin overexpression attenuates ageing-related increase in oxidative stress

A, representative *in situ* immunolabelling of 4-HNE (a marker of oxidative stress) performed in young ($n = 8$) and old ($n = 8$) muscles expressing GFP or overexpressing Parkin. Immunolabelling of whole cross-sections is shown in the first row of images, whereas representative images obtained at a higher magnification are shown in the second row (red scale bars = 1000 μm ; white scale bars = 50 μm). Also shown in (*A*) is the corresponding quantification of 4-HNE immunolabelling intensity, with a strong tendency for an increase in 4-HNE content with ageing and a decrease in 4-HNE content induced by Parkin overexpression in old mice. *B*, western blot detection and quantification of 4-HNE content in the TA of young ($n = 5$) and old ($n = 5$) animals injected with either AAV-Parkin-GFP or AAV-GFP. The data and conclusions obtained by 4-HNE immunolabelling are strengthened. *Statistically significant. [Colour figure can be viewed at wileyonlinelibrary.com]

Parkin overexpression attenuates ageing-related increases in oxidative stress.

Parkin overexpression attenuates ageing-related increase in myonuclear apoptosis

Apoptosis increases significantly in old skeletal muscles and contributes to the development of sarcopenia (Dirks & Leeuwenburgh, 2004; Leeuwenburgh *et al.* 2005; Chabi *et al.* 2008; Gousspillou *et al.* 2014b). We assessed whether Parkin overexpression alters the extent of apoptosis in ageing skeletal muscles. Apoptotic myonuclei were detected in muscle cross-sections using the TUNEL approach combined with DAPI staining and dystrophin immunostaining. As can be seen in Fig. 5, normal

ageing was associated with a significant increase in the number of TUNEL-positive myonuclei (Fig. 5). Parkin overexpression significantly decreased the number of TUNEL-positive myonuclei in old skeletal muscles (Fig. 5).

Parkin overexpression attenuates deposition of type I collagen in old skeletal muscles

Fibrosis develops in old skeletal muscles and contributes to ageing-related declines in skeletal muscle function (Parker *et al.* 2017). The effect of Parkin overexpression on fibrosis inside skeletal muscles was assessed by measuring the content of type I collagen using immunostaining. Normal ageing was associated with a significant increase in muscle type I collagen content (Fig. 6). Parkin

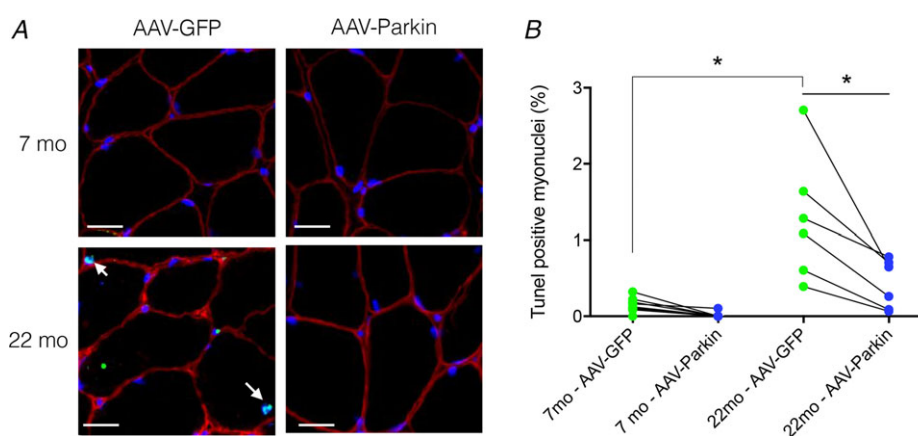


Figure 5. Parkin overexpression attenuates ageing-related increase in myonuclear apoptosis
A, representative TUNEL stain (green; marking apoptotic nuclei) coupled with DAPI staining (blue; marking nuclei) and dystrophin immunolabelling (red) performed in young ($n = 9$) and old ($n = 6$) muscles expressing GFP or overexpressing Parkin. B, quantification of the proportion of TUNEL positive myonuclei showing an increase in apoptosis with ageing and an anti-apoptotic effect of Parkin overexpression (Scale bar = 25 μm). *Statistically significant. [Colour figure can be viewed at wileyonlinelibrary.com]

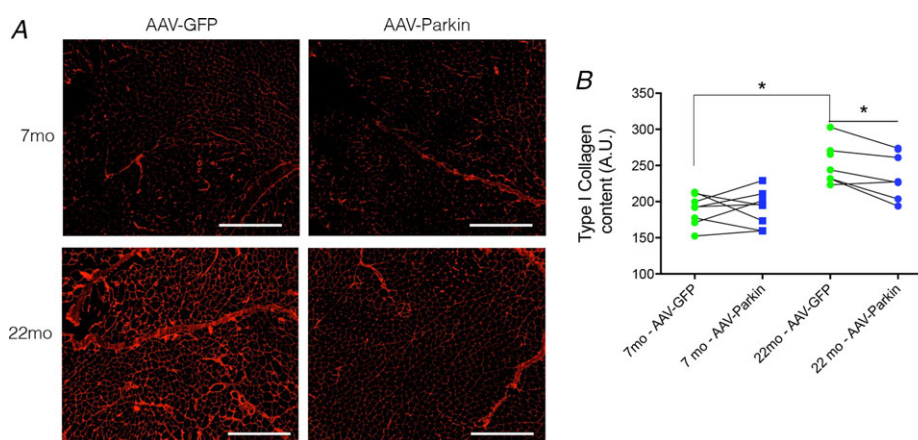


Figure 6. Parkin overexpression attenuates type I collagen deposition in old mice
A, representative type I collagen immunolabelling (red) performed on cross-sections of young ($n = 8$) and old ($n = 7$) muscles expressing GFP or overexpressing Parkin (scale bar = 500 μm). B, type I collagen immunolabelling intensity showing an ageing-related increase in type I collagen content with ageing and a decrease in type I collagen content induced by Parkin overexpression in aged muscles. *Statistically significant. [Colour figure can be viewed at wileyonlinelibrary.com]

overexpression significantly decreased type I collagen content in old but not in young skeletal muscles (Fig. 6). These results indicate that Parkin overexpression attenuates the ageing-related increase in fibrosis in skeletal muscles.

Discussion

Although the aetiology of sarcopenia is extremely complex and only partly understood, the accumulation of mitochondrial dysfunction has been shown to contribute to sarcopenia (Trounce *et al.* 1989; Selman *et al.* 2003; Dirks & Leeuwenburgh, 2004; Leeuwenburgh *et al.* 2005; Short *et al.* 2005; Chabi *et al.* 2008; Marzetti *et al.* 2008; Gousspillou *et al.* 2010; Picard *et al.* 2010; Picard *et al.* 2011; Lanza *et al.* 2012; Umanskaya *et al.* 2014; Gousspillou *et al.* 2014a; Gousspillou *et al.* 2014b). Recent studies have proposed that mitophagic processes controlled by the Parkin–Pink1 pathway may be impaired in aged muscles and are probably responsible for the ageing-related accumulation of dysfunctional mitochondria (O’Leary *et al.* 2013; Rana *et al.* 2013; Gousspillou *et al.* 2014b). On the basis of this proposal, we tested the effect of Parkin overexpression in skeletal muscles of late middle-aged mice on ageing-related loss of muscle mass and strength. The results obtained demonstrate that 4 months of Parkin overexpression in muscles of late-middle aged mice significantly increased muscle mass and strength. These findings provide the proof of principle that increasing Parkin expression just before the appearance of sarcopenia, either through pharmaceutical or non-pharmaceutical means, could represent an effective strategy for attenuating sarcopenia. In this respect, a recent study has shown that supplementing old mice with urolithin A for 27–31 weeks increased their grip strength and endurance (Ryu *et al.* 2016). Although the exact mechanisms by which Urolithin A exerts its beneficial effects in aged mice was not identified, *Park2* (i.e. the gene coding for Parkin) was one of the most upregulated genes upon urolithin A treatment (Ryu *et al.* 2016).

An intriguing observation of the present study is that Parkin overexpression in muscles of young mice triggered hypertrophy. The mechanisms by which Parkin mediates its hypertrophic effects in adult skeletal muscle remain to be fully clarified; our results suggest that Parkin overexpression elicited an increase in the activity of the Akt–mTORC1 pathway, as suggested by the significant increase in phosphorylation of S6 that was observed in mice overexpressing Parkin. The Akt–mTOR pathway is central to the regulation of muscle mass because it promotes protein synthesis and inhibits protein degradation (Schiaffino & Mammucari, 2011). The increase in S6 phosphorylation in response to Parkin overexpression in young muscles is in line with recent

literature indicating that Parkin can ubiquitinate mTOR, a post-translational modification known to increase mTOR activity (Park *et al.* 2014). The lack of impact of Parkin overexpression on S6 phosphorylation suggests that the mechanisms regulating hypertrophy in adult skeletal muscle differ from those involved in the attenuation of sarcopenia.

Amongst the hallmarks of muscle ageing, the presence of oxidative stress is often reported in aged skeletal muscle and has been suggested as a contributing factor to ageing-related declines in muscle mass and function (Yan & Sohal, 1998; Capel *et al.* 2005; Yarian *et al.* 2005; Chabi *et al.* 2008; Sohal & Orr, 2012; Sinha-Hikim *et al.* 2013; Umanskaya *et al.* 2014;). Our results are in line with these observations because we found that aged skeletal muscle demonstrated an increase in 4-HNE content, a marker of oxidative stress. Importantly, 4 months of Parkin overexpression resulted in a significant decrease in 4-HNE content, strongly suggesting that Parkin overexpression attenuated the ageing-related increase in oxidative stress. Although the mechanisms conferring Parkin its protective effects against oxidative stress were not investigated in the present study, it has been shown in p53-depleted pleural cells that Parkin overexpression can increase the glutathione/glutathione disulphide ratio, suggesting that Parkin plays role in the regulation of antioxidant defense systems (Zhang *et al.* 2011).

Another hallmark of muscle ageing is the progressive appearance of fibrosis (Parker *et al.* 2017) and the higher type I collagen content observed in aged muscles in the present study indicates that the old mice developed moderate fibrosis. Such an alteration in muscle connective tissue is assumed to contribute to ageing-related declines in skeletal muscle function (Parker *et al.* 2017). Interestingly, our data show that Parkin overexpression attenuated the ageing-related increase in fibrosis, suggesting that Parkin might play a role in the maintenance of the extracellular matrix. As discussed below, and although the mechanisms underlying this anti-fibrotic effect of Parkin remain to be clarified, we speculate that this anti-fibrotic effect might be linked to the impact of Parkin on apoptosis.

Apoptosis is well known to increase with ageing and contribute to sarcopenia (Dirks & Leeuwenburgh, 2004; Leeuwenburgh *et al.* 2005; Chabi *et al.* 2008; Gousspillou *et al.* 2014b). The present study further reinforces the available literature by showing that aged muscles display an increase in the proportion of TUNEL positive myonuclei, a reliable marker of apoptosis. Importantly, we show that Parkin overexpression significantly attenuated the ageing-related increase in apoptosis. When triggered in skeletal muscle, apoptosis leads to the loss of one or several myonuclei, thereby decreasing the capacity of a muscle fibre for protein synthesis and, ultimately, leading to fibre atrophy (Dupont-Versteegden, 2006).

Prolonged activation of apoptosis can even result in the loss of muscle fibres (Dupont-Versteegden, 2006). The attenuation of apoptosis triggered by Parkin overexpression therefore probably contributed to the higher muscle mass and strength that we measured in old Parkin overexpressing muscles. We also speculate that this anti-apoptotic effect of Parkin might have attenuated fibrosis by preventing the loss of myofibres and their replacement by connective tissue. It is also worth noting that our findings add to the available literature showing that Parkin can exert anti-apoptotic effects (Charan *et al.* 2014).

Another important finding of the present study is the robust increase in mitochondrial content and enzymatic activities that is a result of Parkin overexpression. These findings are in line with a previous study by Rana *et al.* (2013) showing that Parkin overexpression in muscles of *Drosophila melanogaster* resulted in a significant increase in citrate synthase, complex I and complex II enzymatic activities. These findings clearly show that the contribution of Parkin to mitochondrial quality control processes is not limited to mitophagy and extends to mitochondrial biogenesis. Although the underlying mechanisms were not investigated in the present study, the increase in mitochondrial content and enzymatic activities that we observed upon Parkin overexpression was probably mediated by the interaction between Parkin and PARIS. Indeed, it has been recently shown that Parkin can target PARIS, a transcriptional repressor of PGC-1 α , for degradation (Shin *et al.* 2011) and thereby increase mitochondrial biogenesis. The increase in mitochondrial content and enzymatic activities caused by Parkin overexpression indicates that Parkin can positively impact skeletal muscle energy metabolism.

Declining PGC-1 α expression with ageing has been proposed as a contributing factor to explain ageing-related loss of muscle mass and function (Dillon *et al.* 2012). In the present study, we show that Parkin overexpression in old muscle attenuated the ageing-related decline in PGC-1 α content. Considering the fact that PGC-1 α overexpression has been shown to partly attenuate ageing-related loss of fibre size (Garcia *et al.* 2018), it is possible that some of the anti-ageing effects of Parkin overexpression were mediated by its impact on PGC-1 α content in old muscles.

Recent studies have provided evidence that Parkin is involved in the regulation of mitochondrial dynamics and morphology. Indeed, Parkin can ubiquitinate the pro-fusion proteins Mfn2 and Mfn1, thereby targeting these proteins for proteosomal degradation (Gegg *et al.* 2010). The degradation of these pro-fusion proteins is considered to tip the fusion/fission balance towards mitochondrial fission (Gegg *et al.* 2010). In line with this view, Parkin overexpression in fly skeletal muscle and in rat hippocampal neurons has been shown to stimulate mitochondrial fragmentation (Yu *et al.* 2011;

Rana *et al.* 2013). The results of the present further strengthen this literature because we show that Parkin overexpression in old muscle decreased the average area of individual intermyofibrillar mitochondria, therefore suggesting mitochondrial fragmentation. Interestingly, we have recently shown that skeletal muscle ageing is associated with an enlargement of subsarcolemmal mitochondria and an increase in the morphological complexity (increased branching and length) of intermyofibrillar mitochondria (Leduc-Gaudet *et al.* 2015). Our data suggest that Parkin overexpression might have attenuated the effects of ageing on mitochondrial morphology and dynamics. Because mitophagy of large mitochondria requires their fission (Twig & Shirihai, 2011), it is tempting to speculate that the smaller mitochondria seen in old Parkin overexpressing muscles might facilitate their recycling when they become damaged/dysfunctional. Combined with the documented positive effect of Parkin overexpression on mitochondrial biogenesis, mitochondrial fragmentation caused by Parkin overexpression might help in the maintenance of a healthy pool of mitochondria throughout ageing.

In conclusion, the present study shows that Parkin overexpression attenuates ageing-related loss of muscle mass and strength and causes hypertrophy in adult skeletal muscles. In addition, our results show that Parkin overexpression leads to increases in mitochondrial content and enzymatic activities. Finally, our findings indicate that Parkin overexpression attenuates ageing-related increases in markers of oxidative stress, fibrosis and apoptosis. These results place Parkin as a potential therapeutic target for attenuating sarcopenia and improving skeletal muscle health and performance.

References

- Allen DG, Lamb GD & Westerblad H (2008). Skeletal muscle fatigue: cellular mechanisms. *Physiol Rev* **88**, 287–332.
- Baker DJ, Betik AC, Krause DJ & Hepple RT (2006). No decline in skeletal muscle oxidative capacity with aging in long-term calorically restricted rats: effects are independent of mitochondrial DNA integrity. *J Gerontol A Biol Sci Med Sci* **61**, 675–684.
- Benjamini Y, Krieger AM & Yekutieli D (2006). Adaptive linear step-up procedures that control the false discovery rate. *Biometrika* **93**, 491–507.
- Capel F, Rimbart V, Lioger D, Diot A, Rousset P, Mirand PP, Boirie Y, Morio B & Mosoni L (2005). Due to reverse electron transfer, mitochondrial H₂O₂ release increases with age in human vastus lateralis muscle although oxidative capacity is preserved. *Mech Ageing Dev* **126**, 505–511.
- Carnio S, LoVerso F, Baraibar MA, Longa E, Khan MM, Maffei M, Reischl M, Canepari M, Loeffler S, Kern H, Blaauw B, Friguet B, Bottinelli R, Rudolf R & Sandri M (2014). Autophagy impairment in muscle induces neuromuscular junction degeneration and precocious aging. *Cell Rep* **8**, 1509–1521.

- Chabi B, Ljubic V, Menzies KJ, Huang JH, Saleem A & Hood DA (2008). Mitochondrial function and apoptotic susceptibility in aging skeletal muscle. *Aging Cell* **7**, 2–12.
- Charan RA, Johnson BN, Zaganelli S, Nardozi JD & LaVoie MJ (2014). Inhibition of apoptotic Bax translocation to the mitochondria is a central function of parkin. *Cell Death Dis* **5**, e1313.
- Coggan AR, Spina RJ, King DS, Rogers MA, Brown M, Nemeth PM & Holloszy JO (1992). Skeletal muscle adaptations to endurance training in 60- to 70-yr-old men and women. *J Appl Physiol* (1985) **72**, 1780–1786.
- Deschenes MR (2004). Effects of aging on muscle fibre type and size. *Sports Med* **34**, 809–824.
- Dillon LM, Rebelo AP & Moraes CT (2012). The role of PGC-1 coactivators in aging skeletal muscle and heart. *IUBMB Life* **64**, 231–241.
- Dirks AJ & Leeuwenburgh C (2004). Aging and lifelong caloric restriction result in adaptations of skeletal muscle apoptosis repressor, apoptosis-inducing factor, X-linked inhibitor of apoptosis, caspase-3, and caspase-12. *Free Radic Biol Med* **36**, 27–39.
- Drummond MJ, Addison O, Brunker L, Hopkins PN, McClain DA, LaStayo PC & Marcus RL (2014). Downregulation of E3 ubiquitin ligases and mitophagy-related genes in skeletal muscle of physically inactive, frail older women: a cross-sectional comparison. *J Gerontol A Biol Sci Med Sci* **69**, 1040–1048.
- Dupont-Versteegden EE (2006). Apoptosis in skeletal muscle and its relevance to atrophy. *World J Gastroenterol* **12**, 7463.
- Garcia S, Nissanka N, Mareco EA, Rossi S, Peralta S, Diaz F, Rotundo RL, Carvalho RF & Moraes CT (2018). Overexpression of PGC-1 α in aging muscle enhances a subset of young-like molecular patterns. *Aging Cell* **17**.
- Gegg ME, Cooper JM, Chau KY, Rojo M, Schapira AH & Taanman JW (2010). Mitofusin 1 and mitofusin 2 are ubiquitinated in a PINK1/parkin-dependent manner upon induction of mitophagy. *Hum Mol Genet* **19**, 4861–4870.
- Gospillou G, Sgarioto N, Norris B, Barbat-Artigas S, Aubertin-Leheudre M, Morais JA, Burelle Y, Taivassalo T & Hepple RT (2014c). The relationship between muscle fiber type-specific PGC-1 α content and mitochondrial content varies between rodent models and humans. *PLoS ONE* **9**, e103044.
- Gospillou G, Bourdel-Marchasson I, Rouland R, Calmettes G, Biran M, Deschodt-Arsac V, Miraux S, Thiaudiere E, Pasdois P, Detaille D, Franconi JM, Babot M, Trezeguet V, Arsac L & Diolez P (2014a). Mitochondrial energetics is impaired in vivo in aged skeletal muscle. *Aging Cell* **13**, 39–48.
- Gospillou G, Bourdel-Marchasson I, Rouland R, Calmettes G, Franconi JM, Deschodt-Arsac V & Diolez P (2010). Alteration of mitochondrial oxidative phosphorylation in aged skeletal muscle involves modification of adenine nucleotide translocator. *Biochim Biophys Acta* **1797**, 143–151.
- Gospillou G, Godin R, Piquereau J, Picard M, Mofarrahi M, Mathew J, Purves-Smith FM, Sgarioto N, Hepple RT, Burelle Y & Hussain SN (2018). Protective role of Parkin in skeletal muscle contractile and mitochondrial function. *J Physiol*.
- Gospillou G & Hepple RT (2013). Facts and controversies in our understanding of how caloric restriction impacts the mitochondrion. *Exp Gerontol* **48**, 1075–1084.
- Gospillou G, Sgarioto N, Kapchinsky S, Purves-Smith F, Norris B, Pion CH, Barbat-Artigas S, Lemieux F, Taivassalo T, Morais JA, Aubertin-Leheudre M & Hepple RT (2014b). Increased sensitivity to mitochondrial permeability transition and myonuclear translocation of endonuclease G in atrophied muscle of physically active older humans. *FASEB J* **28**, 1621–1633.
- Grundy D (2015). Principles and standards for reporting animal experiments in The Journal of Physiology and Experimental Physiology. *J Physiol* **593**, 2547–2549.
- Hepple RT, Baker DJ, McConkey M, Murynka T & Norris R (2006). Caloric restriction protects mitochondrial function with aging in skeletal and cardiac muscles. *Rejuvenation Res* **9**, 219–222.
- Hwee DT, Baehr LM, Philp A, Baar K & Bodine SC (2014). Maintenance of muscle mass and load-induced growth in Muscle RING Finger 1 null mice with age. *Aging Cell* **13**, 92–101.
- Janssen I, Baumgartner RN, Ross R, Rosenberg IH & Roubenoff R (2004a). Skeletal muscle cutpoints associated with elevated physical disability risk in older men and women. *Am J Epidemiol* **159**, 413–421.
- Janssen I, Heymsfield SB & Ross R (2002). Low relative skeletal muscle mass (sarcopenia) in older persons is associated with functional impairment and physical disability. *J Am Geriatr Soc* **50**, 889–896.
- Janssen I, Shepard DS, Katzmarzyk PT & Roubenoff R (2004b). The healthcare costs of sarcopenia in the United States. *J Am Geriatr Soc* **52**, 80–85.
- Joseph AM, Adhietty PJ, Buford TW, Wohlgenuth SE, Lees HA, Nguyen LM, Aranda JM, Sandesara BD, Pahor M, Manini TM, Marzetti E & Leeuwenburgh C (2012). The impact of aging on mitochondrial function and biogenesis pathways in skeletal muscle of sedentary high- and low-functioning elderly individuals. *Aging Cell* **11**, 801–809.
- Kim TN & Choi KM (2013). Sarcopenia: definition, epidemiology, and pathophysiology. *J Bone Metab* **20**, 1–10.
- Kyrylkova K, Kyryachenko S, Leid M & Kioussi C (2012). Detection of apoptosis by TUNEL assay. *Methods Mol Biol* **887**, 41–47.
- Lanza IR, Zabielski P, Klaus KA, Morse DM, Heppelmann CJ, Bergen HR, 3rd, Dasari S, Walrand S, Short KR, Johnson ML, Robinson MM, Schimke JM, Jakaitis DR, Asmann YW, Sun Z & Nair KS (2012). Chronic caloric restriction preserves mitochondrial function in senescence without increasing mitochondrial biogenesis. *Cell Metab* **16**, 777–788.
- Leduc-Gaudet JP, Picard M, St-Jean Pelletier F, Sgarioto N, Auger MJ, Vallee J, Robitaille R, St-Pierre DH & Gospillou G (2015). Mitochondrial morphology is altered in atrophied skeletal muscle of aged mice. *Oncotarget* **6**, 17923–17937.
- Leeuwenburgh C, Gurley CM, Strotman BA & Dupont-Versteegden EE (2005). Age-related differences in apoptosis with disuse atrophy in soleus muscle. *Am J Physiol Regul Integr Comp Physiol* **288**, R1288–R1296.

- Marzetti E, Wohlge-muth SE, Lees HA, Chung HY, Giovannini S & Leeuwenburgh C (2008). Age-related activation of mitochondrial caspase-independent apoptotic signaling in rat gastrocnemius muscle. *Mech Ageing Dev* **129**, 542–549.
- Masiero E, Agatea L, Mammucari C, Blaauw B, Loro E, Komatsu M, Metzger D, Reggiani C, Schiaffino S & Sandri M (2009). Autophagy is required to maintain muscle mass. *Cell Metab* **10**, 507–515.
- Mayhew M, Renganathan M & Delbono O (1998). Effectiveness of caloric restriction in preventing age-related changes in rat skeletal muscle. *Biochem Biophys Res Commun* **251**, 95–99.
- Mofarrahi M, McClung JM, Kontos CD, Davis EC, Tappuni B, Moroz N, Pickett AE, Huck L, Harel S, Danialou G & Hussain SN (2015). Angiopoietin-1 enhances skeletal muscle regeneration in mice. *Am J Physiol Regul Integr Comp Physiol* **308**, R576–R589.
- Narendra D, Tanaka A, Suen DF & Youle RJ (2008). Parkin is recruited selectively to impaired mitochondria and promotes their autophagy. *J Cell Biol* **183**, 795–803.
- O’Leary MF, Vainshtein A, Iqbal S, Ostojic O & Hood DA (2013). Adaptive plasticity of autophagic proteins to denervation in aging skeletal muscle. *Am J Physiol Cell Physiol* **304**, C422–C430.
- Park D, Lee MN, Jeong H, Koh A, Yang YR, Suh PG & Ryu SH (2014). Parkin ubiquitinates mTOR to regulate mTORC1 activity under mitochondrial stress. *Cell Signal* **26**, 2122–2130.
- Parker L, Caldwell MK, Watts R, Levinger P, Cameron-Smith D & Levinger I (2017). Age and sex differences in human skeletal muscle fibrosis markers and transforming growth factor-beta signaling. *Eur J Appl Physiol* **117**, 1463–1472.
- Picard M, Gentil BJ, McManus MJ, White K, Louis KS, Gartside SE, Wallace DC & Turnbull DM (2013a). Acute exercise remodels mitochondrial membrane interactions in mouse skeletal muscle. *J Appl Physiol* **115**, 1562–1571.
- Picard M, Ritchie D, Thomas MM, Wright KJ & Hepple RT (2011). Alterations in intrinsic mitochondrial function with aging are fiber type-specific and do not explain differential atrophy between muscles. *Ageing Cell* **10**, 1047–1055.
- Picard M, Ritchie D, Wright KJ, Romestaing C, Thomas MM, Rowan SL, Taivassalo T & Hepple RT (2010). Mitochondrial functional impairment with aging is exaggerated in isolated mitochondria compared to permeabilized myofibers. *Ageing Cell* **9**, 1032–1046.
- Picard M, White K & Turnbull DM (2013b). Mitochondrial morphology, topology, and membrane interactions in skeletal muscle: a quantitative three-dimensional electron microscopy study. *J Appl Physiol* **114**, 161–171.
- Rana A, Rera M & Walker DW (2013). Parkin overexpression during aging reduces proteotoxicity, alters mitochondrial dynamics, and extends lifespan. *Proc Natl Acad Sci U S A* **110**, 8638–8643.
- Ryu D, Mouchiroud L, Andreux PA, Katsyuba E, Moullan N, Nicolet-Dit-Felix AA, Williams EG, Jha P, Lo Sasso G, Huzard D, Aebischer P, Sandi C, Rinsch C & Auwerx J (2016). Urolithin A induces mitophagy and prolongs lifespan in *C. elegans* and increases muscle function in rodents. *Nat Med* **22**, 879–888.
- Santilli V, Bernetti A, Mangone M & Paoloni M (2014). Clinical definition of sarcopenia. *Clin Cases Miner Bone Metab* **11**, 177–180.
- Schiaffino S & Mammucari C (2011). Regulation of skeletal muscle growth by the IGF1-Akt/PKB pathway: insights from genetic models. *Skelet Muscle* **1**, 4.
- Selman C, Gredilla R, Phaneuf S, Kendaiah S, Barja G & Leeuwenburgh C (2003). Short-term caloric restriction and regulatory proteins of apoptosis in heart, skeletal muscle and kidney of Fischer 344 rats. *Biogerontology* **4**, 141–147.
- Shin JH, Ko HS, Kang H, Lee Y, Lee YI, Pletinkova O, Troconso JC, Dawson VL & Dawson TM (2011). PARIS (ZNF746) repression of PGC-1 α contributes to neurodegeneration in Parkinson’s disease. *Cell* **144**, 689–702.
- Short KR, Bigelow ML, Kahl J, Singh R, Coenen-Schimke J, Raghavakaimal S & Nair KS (2005). Decline in skeletal muscle mitochondrial function with aging in humans. *PNAS* **102**, 5618–5623.
- Sinha-Hikim I, Sinha-Hikim AP, Parveen M, Shen R, Goswami R, Tran P, Crum A & Norris KC (2013). Long-term supplementation with a cystine-based antioxidant delays loss of muscle mass in aging. *J Gerontol A Biol Sci Med Sci* **68**, 749–759.
- Sohal RS & Orr WC (2012). The redox stress hypothesis of aging. *Free Radic Biol Med* **52**, 539–555.
- Song W, Kwak HB & Lawler JM (2006). Exercise training attenuates age-induced changes in apoptotic signaling in rat skeletal muscle. *Antioxid Redox Signal* **8**, 517–528.
- St-Jean-Pelletier F, Pion CH, Leduc-Gaudet JP, Sgarioto N, Zovile I, Barbat-Artigas S, Reynaud O, Alkaterji F, Lemieux FC, Grenon A, Gaudreau P, Hepple RT, Chevalier S, Belanger M, Morais JA, Aubertin-Leheudre M & Gousspillou G (2017). The impact of ageing, physical activity, and pre-frailty on skeletal muscle phenotype, mitochondrial content, and intramyocellular lipids in men. *J Cachexia Sarcopenia Muscle* **8**, 213–228.
- Sun Y, Vashisht AA, Tchiew J, Wohlschlegel JA & Dreier L (2012). Voltage-dependent anion channels (VDACs) recruit Parkin to defective mitochondria to promote mitochondrial autophagy. *J Biol Chem* **287**, 40652–40660.
- Tieland M, Trouwborst I & Clark BC (2018). Skeletal muscle performance and ageing. *J Cachexia Sarcopenia Muscle* **9**, 3–19.
- Trounce I, Byrne E & Marzuki S (1989). Decline in skeletal muscle mitochondrial respiratory chain function: possible factor in ageing. *Lancet* **1**, 637–639.
- Twig G & Shirihai OS (2011). The interplay between mitochondrial dynamics and mitophagy. *Antioxid Redox Signal* **14**, 1939–1951.
- Umanskaya A, Santulli G, Xie W, Andersson DC, Reiken SR & Marks AR (2014). Genetically enhancing mitochondrial antioxidant activity improves muscle function in aging. *Proc Natl Acad Sci U S A* **111**, 15250–15255.
- Yan LJ & Sohal RS (1998). Mitochondrial adenine nucleotide translocase is modified oxidatively during aging. *Proc Natl Acad Sci U S A* **95**, 12896–12901.
- Yarian CS, Rebrin I & Sohal RS (2005). Aconitase and ATP synthase are targets of malondialdehyde modification and undergo an age-related decrease in activity in mouse heart

mitochondria. *Biochem Biophys Res Commun* **330**, 151–156.

Yu W, Sun Y, Guo S & Lu B (2011). The PINK1/Parkin pathway regulates mitochondrial dynamics and function in mammalian hippocampal and dopaminergic neurons. *Hum Mol Genet* **20**, 3227–3240.

Zhang C, Lin M, Wu R, Wang X, Yang B, Levine AJ, Hu W & Feng Z (2011). Parkin, a p53 target gene, mediates the role of p53 in glucose metabolism and the Warburg effect. *Proc Natl Acad Sci U S A* **108**, 16259–16264.

Additional information

Competing interests

The authors declare that they have no competing interests.

Author contributions

GG and SH designed and conceived the study. JPLG, OR and GG collected and analysed the data. All authors interpreted

the data and contributed to the writing of the manuscript. All authors approved the final version of the manuscript submitted for publication.

Funding

This work was funded by grants from the Natural Sciences and Engineering Council of Canada (NSERC) awarded to Gilles Gouspillou (#RGPIN-2014-04668) and from the Canadian Institute of Health Research (CIHR; MOP-93760) awarded to Sabah N. A. Hussain. Gilles Gouspillou is also supported by a Chercheur Boursier Junior 1 salary award from the Fonds de Recherche du Québec en Santé (FRQS-35184). Jean-Philippe Leduc-Gaudet is supported by a CIHR Vanier Fellowship. The funders had no role in the study design, data collection and analysis, decision to publish, or preparation of the manuscript.